

The Southern Sky Redshift Survey ¹

L. Nicolaci da Costa,²

European Southern Observatory, Karl Schwarzschild Str. 2, 85748 Garching-bei-München,
Germany

C. N. A. Willmer, P.S. Pellegrini, O. L. Chaves, C. Rit e, M. A. G. Maia

Departamento de Astronomia, Observat rio Nacional, Rua General Jos  Cristino 77, Rio de
Janeiro, 20921-030, Brazil

M.J. Geller, D.W. Latham, M.J. Kurtz, J.P. Huchra

Harvard-Smithsonian Center for Astrophysics, 60 Garden St., Cambridge MA 02138

M. Ramella,

Osservatorio Astronomico di Trieste, Via G. B. Tiepolo 11, 34131 Trieste, Italy

A.P. Fairall,

Department of Astronomy, University of Cape Town, 7735 Rondebosch, South Africa

C. Smith,

Department of Astronomy, University of Michigan, Ann Arbor, MI

and

S. L ipari

Observatorio Astron mico de C rdoba, Laprida 854, C rdoba, 5000, Argentina

ABSTRACT

We report redshifts, magnitudes and morphological classifications for 5369 galaxies with $m_B \leq 15.5$ and 57 galaxies fainter than this limit, in two regions covering a total of 1.70 steradians in the southern celestial hemisphere. The galaxy catalog is drawn primarily from the list of non-stellar objects identified in the Guide Star

¹Based on observations at Cerro Tololo Interamerican Observatory (CTIO), National Optical Astronomy Observatories (NOAO) which is operated by the Association of Universities for Research in Astronomy, Inc. under contract to the National Science Foundation; Complejo Astronomico El Leoncito (CASLEO), operated under agreement between the Consejo Nacional de Investigaciones Cient ficas de la Rep blica Argentina and the National Universities of La Plata, C rdoba and San Juan; European Southern Observatory (ESO), partially under the bilateral agreement ESO-ON; Fred Lawrence Whipple Observatory; Laborat rio Nacional de Astrof sica; and the South African Astronomical Observatory

²Departamento de Astronomia, Observat rio Nacional, Rua General Jos  Cristino 77, Rio de Janeiro, 20921-030, Brazil

Catalog (Lasker et al. 1990, AJ 99, 2019; hereafter GSC). The galaxies have positions accurate to $\sim 1''$ and magnitudes with an rms scatter of $\sim 0.3^m$. We compute magnitudes (m_{SSRS2}) from the relation between instrumental GSC magnitudes and the photometry by Lauberts & Valentijn (1989). From a comparison with CCD photometry, we find that our system is homogeneous across the sky and corresponds to magnitudes measured at the isophotal level $\sim 26 \text{ mag arcsec}^{-2}$. The precision of the radial velocities is of $\sim 40 \text{ kms}^{-1}$ and the redshift survey is more than 99% complete to the $m_{SSRS2} = 15.5$ magnitude limit. This sample is in the direction opposite to the CfA2; in combination the two surveys provide an important database for studies of the properties of galaxies and their large-scale distribution in the nearby Universe.

Subject headings: Galaxies: distances and redshifts – galaxies: photometry

1. Introduction

During the past two decades, complete, wide-angle redshift surveys have provided a fundamental basis for exploring the large-scale distribution of galaxies. Starting with the CfA1 Redshift Survey (Davis et al. 1982), the first to reach beyond the Local Supercluster, these surveys have revolutionized our view of the spatial distribution of galaxies. The CfA1 redshift survey provided the first three-dimensional glimpse of the nearby universe, showing that within $70h^{-1}$ Mpc ($H_0 = 100h^{-1}$ km/s/Mpc) the galaxy distribution is far from homogeneous with large regions devoid of bright objects. The first complete slice of the CfA2 Redshift Survey (de Lapparent et al. 1986) soon produced striking results with the discovery of the Great Wall, a spectacular example of a well-defined, thin, two-dimensional structure perpendicular to the line-of-sight and outlining several large voids (de Lapparent et al. 1986). Later the diameter-limited Southern Sky Redshift Survey (SSRS, da Costa et al. 1988), not only confirmed the existence of large voids, but also detected other thin two-dimensional coherent structures, like the Southern wall. These surveys revealed the large scale of structure in the universe.

Surveys of both hemispheres have continued: the CfA2 covers a portion of both galactic caps in the northern celestial hemisphere (Geller & Huchra 1989) and the SSRS2 (*e.g.*, da Costa et al. 1994a) covers a portion of both caps in the south. In contrast to the diameter-limited SSRS, the deeper SSRS2 is a magnitude limited survey based on a selection of objects from the Hubble Space Telescope Guide Star Catalog (Lasker et al. 1990; GSC hereafter).

The CfA2 and SSRS2 surveys now cover more than 30% of the sky. Together they contain more than 20,000 galaxies and provide a panoramic view of the three-dimensional galaxy distribution (*e.g.*, da Costa et al. 1994a). The redshift survey maps show that the galaxy distribution consists of a complex network of voids, typically 5000 kms^{-1} in size, surrounded by thin walls where most galaxies reside (Geller & Huchra 1989). A quantitative analysis of the SSRS2 (El-ad et al. 1996) confirms this picture, finding the typical size of voids to be $\sim 40h^{-1}$ Mpc. Contrary to some earlier expectations, large voids and walls are not rare events; they are present in every direction surveyed (*e.g.*, CfA2; Las Campanas Redshift Survey, Schectman et al. 1996).

Both separately and combined, the CfA2 and SSRS2 have provided a basis for determination of the local luminosity function (Marzke et al. 1994b, da Costa et al. 1994a) and its dependence on morphology (Marzke et al. 1994a, Marzke et al. 1998) and color (Marzke & da Costa 1997); the power-spectrum of the galaxy distribution (Park et al. 1994, da Costa et al. 1994b); the mean pairwise velocity dispersion (Marzke et al. 1995); the dependence of clustering properties on luminosity (Benoist et al. 1996), morphology and color (Willmer et al. 1998) and the properties of loose and compact groups (Barton et al. 1996, Ramella et al. 1997, Ramella et al. 1998).

Even though the currently planned deeper surveys will dramatically extend the depth of the sampled volume of the Universe, the combined CfA2 and SSRS2, which probe the distribution of L_* galaxies out to $\sim 100 h^{-1}$ Mpc, will continue to be a valuable database. For instance,

the large number of galaxies, the complete sampling and the large angular coverage will allow, in conjunction with independent distance measurements, a more detailed study of the relation between individual galaxies and large-scale structure.

Here we provide the SSRS2 catalog. In Section 2 we discuss the assembly of the sample of galaxies from the GSC, the magnitude system, and the morphological classification of galaxies. In Section 3 we describe the observations. The catalog itself is in Section 4. A brief summary follows in Section 5.

2. The Sample

2.1. Constructing the catalog

We selected the SSRS2 galaxy sample from the list of non-stellar objects in the GSC. The sample covers the region $-40^\circ \leq \delta \leq -2.5^\circ$ and $b \leq -40^\circ$ in the Southern Galactic cap (SSRS2 south), and the region $\delta \leq 0^\circ$ and $b \geq +35^\circ$ in the Northern Galactic cap (SSRS2 north). The northern limits in declination make the SSRS2 contiguous with the CfA2.

The GSC has good astrometric accuracy ($\sim 1''$) and objectively measured instrumental magnitudes. To examine the adequacy of the instrumental GSC magnitudes, we identified the GSC counterparts for about 1000 galaxies from the Lauberts and Valentijn (1989, hereafter ESO-LV) catalog, and compared the instrumental and ESO-LV magnitudes. We find a linear relation with small scatter ($\approx 0.3^m$) between these magnitudes. This relation yields a transformation between the GSC instrumental magnitudes and the ESO-LV measurements (Alonso et al. 1993). Using this relation (see Section 2.2) we extracted a preliminary sample of objects from the GSC with $m_{ssrs2} \leq 15.5$.

The “non-stellar” GSC list includes many visual double or triple stars, parts of bright galaxies, and satellite and asteroid trails. Thus it is not possible to equate all “non-stellar” objects with galaxies. To identify the galaxies in this preliminary sample, we either matched the list with other known galaxy catalogs or visually inspected the images. The typical number of “non-stellar” objects in a 10° declination strip of the GSC, within the survey boundaries, is ~ 5500 ; only 900 ($\sim 16\%$) of these are galaxies.

To investigate the nature of the selected objects, we matched the list with the following series of galaxy catalogues: 1) The ESO-LV catalog yielded 1477 galaxies in common with the SSRS2 south and 338 in the SSRS2 north for declinations $\delta \leq -17.5^\circ$, the northern limit of the ESO-LV catalog. For a match, we required a separation $\lesssim 3'$; 2) For declinations $\delta > -17.5^\circ$ we matched the sample with the Morphological Catalogue of Galaxies (Vorontsov-Velyaminov & Arkhipova 1963-1968, hereafter MCG) allowing separations $\leq 4'$ (because of the large errors in the catalog coordinates) to find 900 matches in the SSRS2 south and 837 in the SSRS2 north; 3) We then matched the remaining objects to a subset of the APM survey with $m_B \lesssim 16$ (Loveday 1996) in the

southern galactic cap ($-40^\circ \leq \delta \leq -2.5^\circ$, kindly provided by S. Maddox and W. Sutherland). We cross-identified ~ 700 APM galaxies. For the SSRS2 north, a similar match to an APM catalog (Raychaudhuri et al. 1994, kindly provided by Somak Raychaudhuri) yielded ~ 580 matches.

Taken together the matching procedures identified $\sim 88\%$ of the galaxies in the final catalog. The matching procedure also showed that galaxies with very large apparent diameters are not included in the GSC, but can be found in either the ESO-LV or the MCG. In these cases, we used the coordinates from the parent catalog and converted the magnitudes using the appropriate relation (see Section 2.2). We recover 124 galaxies from the ESO-LV and 173 from the MCG. These large objects are missing in the APM catalog as well as in the GSC ; both suffer from the same bias. These cases constitute $\sim 6\%$ of the sample.

Finally, we visually inspected the remaining unmatched objects in the preliminary GSC "non-stellar" list. We identified ~ 190 galaxies in the southern and 100 in the northern subsamples accounting for $\sim 6\%$ of the final sample. Visual inspection revealed that a few (~ 30) bright and single galaxies were split in the GSC into two or more components. In these cases we maintained the object as a single entry in the catalog and used magnitudes from the ESO-LV or MCG catalogs, converted into the m_{SSRS2} system (Section 2.2). Visual inspection also showed that quite often close pairs of galaxies (especially galaxies classified as "interacting galaxies" (IG) by Lauberts (1982)) appear as a single object in the GSC. If we had detailed information for each galaxy from the ESO-LV (coordinates, magnitudes and velocities) we used it to split the GSC entry into the appropriate number of galaxies, with appropriate coordinates and magnitudes converted to the m_{SSRS2} system. In cases where data for the separate galaxies were unavailable, we estimated the magnitudes. For about 16 galaxies, the estimated magnitude was brighter than our magnitude limit and new entries were created in the catalog, and new coordinates measured. We believe that this careful inspection insures the completeness of the catalog to the desired limiting magnitude.

As a final note, we point out that some galaxies may still be missed depending on the performance of the galaxy/star classification algorithm used by the GSC. In order to evaluate this effect we searched for APM galaxies in the GSC "stellar" list, finding that about half of the matches had already been included in the SSRS2 catalog from our searches in the ESO and MCG catalogs. The results indicate that our incompleteness, due to the misclassification of galaxies as stars, is $\lesssim 2\%$, occurring primarily in the fainter 0.5 magnitude bin.

2.2. Magnitudes

The SSRS2 magnitude system converts the GSC instrumental magnitudes to the magnitude system of the ESO-LV catalog. About 1000 GSC "non-stellar" objects matched to ESO-LV galaxies determine the linear relation between the GSC instrumental magnitudes, m_{GSC} and ESO-LV B_T magnitudes. We then add a constant term to these B_T magnitudes to match the Zwicky-B(0) (Huchra 1976; de Vaucouleurs & de Vaucouleurs 1964) system of the CfA2. From

Felten (1985), we take a constant term of 0.26^m . The relationship between m_{SSRS2} and m_{GSC} is then (Alonso et al. 1993)

$$m_{SSRS2} = 0.59 m_{GSC} + 8.42 \quad (1)$$

A comparison of the m_{SSRS2} magnitudes with CCD photometry (Alonso et al. 1993, 1994) shows that the m_{SSRS2} 's have a limiting isophotal level close to 26 mag arcsec⁻². The rms uncertainty in the magnitudes is $\sim 0.30^m$. Alonso et al. (1994) also verify that the photometry is uniform across the survey. They found a mean offset $m_B(26) - m_{SSRS2} = -0.02$; the variation of the zero-point over the sky is $\sim \pm 0.10$ magnitudes for regions at large angular separations. From a small number of galaxies for which both m_{SSRS2} and m_{Zwicky} are available, Alonso et al. (1994) also show that the zero-point offset is $m_{SSRS2} - m_{Zwicky} \sim 0.10^m$, smaller than the typical magnitude errors in either catalog (0.35^m for m_{Zwicky}).

To further justify the above results in figure 1 we compare m_{SSRS2} magnitudes, as defined above, with B_{26} taken from the ESO-LV for 1588 galaxies in common. In the figure, we also show the linear χ^2 fit obtained in the domain $13 \leq m_{SSRS2} \leq 15.5$, which yields the relation $B_{26} = 1.01 m_{SSRS2} - 0.10$, with a dispersion of about 0.33^m . Assuming the errors in B_{26} to be $\sim 0.1^m$, we estimate the errors in m_{SSRS2} to be about 0.31^m , confirming the findings of Alonso et al. (1994), for a much larger sample of galaxies.

For single objects which were split in the GSC, or for two or more galaxies with a single entry in the GSC, we use magnitudes tabulated in the ESO-LV or MCG catalogs converted into m_{SSRS2} by adding 0.26^m to the ESO-LV B_T or by adding 0.5^m to the MCG magnitude. For merged images not separated by the GSC, and not contained in the ESO-LV nor in the MCG, we use the GSC magnitude to obtain m_{SSRS2} , as given by equation (1), rather than including a visual estimate.

Figure 2 shows the number counts of galaxies in 0.5 magnitude intervals for both subsamples (North and South) of the SSRS2. Although there are small sample fluctuations for bright galaxies ($m_{SSRS2} \lesssim 11$), the counts for the two subsamples are in excellent agreement at fainter magnitudes and both have a slope of ~ 0.6 . There is no flattening of the slope at the faintest magnitudes, indicating that there is no significant loss of objects at the limit of the survey.

2.3. Morphology

Although the visual classification of a “non-stellar” object as a galaxy is straightforward, the morphological classification is not (*e.g.*, Lahav et al. 1995); classifications vary from individual to individual. In the SSRS2 catalog, we include morphological classifications for all galaxies available in the ESO-LV for $\delta \leq -17.5^\circ$ (1815 galaxies); from the ZCAT compilation of Huchra (1996, private communication); and from an APM classification (W. Sutherland, private communication) in the declination range $-10^\circ \leq \delta \leq -2.5^\circ$ for the southern galactic cap only.

The ESO-LV morphology is the most detailed and homogeneous classification, subdivided into

transition types and subclasses, and we adopt it as our reference system. The APM classification includes only principal types and we transform them into T types: ellipticals (T=-5), S0s (T=-2), spirals (T=5), and irregulars (T=10). ZCAT morphologies are not so homogeneous as the other catalogs because it is a compilation which includes data from several sources. We also map these classifications to conform with the ESO-LV system. We point out, however, that while in the ESO-LV system, T=5 corresponds to generic spirals, here we have assigned this type for all spirals pending more detailed classification. We also devised numerical codes for peculiar galaxies (T=15) and unclassified objects (T=23).

To provide complete morphological information, we visually inspected galaxies with no previous classification. To calibrate our classifications and to make them as consistent as possible with the ESO-LV system we re-classified galaxies in the ESO-LV without looking at the published T type. For the SSRS2 south we used film copies of the ESO(B) Atlas and, in doubtful cases, we also used the ESO-SRC (J) film copies. By iteratively classifying and checking, we became confident in our classifications when they matched the ESO-LV more than 85% of the time. Most of the discrepancies come from misclassifying S0s, either as ellipticals or as early spirals. We then used the ESO (B) film copies to classify objects south of declination $\delta = -17.5^\circ$; northward of this limit we used paper copies of the Palomar Observatory Sky Survey (POSS). For the SSRS2 north, which was examined later, we used the Digitized Sky Survey. The lower photographic quality of the POSS paper copies may have led us to misclassify some early spirals as S0s or even ellipticals. However, we classified only about 200 galaxies ($\sim 4\%$ of the sample) from the POSS.

We emphasize that our system of morphological types is only homogeneous and complete when coarsely binned, *i.e.*, if we define ellipticals as T=[-5 to -3], lenticulars as T=[-2 to 0], and spirals as T=[1 to 9]. Adopting this definition we find that the magnitude-limited SSRS2 consists of: 12.5% of ellipticals, 19.0% of S0s, 64.0% of spirals, 1.5% of irregulars, 2.6% of peculiars and 0.4% of unclassified galaxies. More recently we began using images from the Digitized Sky Survey and the process of classifying all objects with greater morphological resolution is underway. We will periodically update the catalog version available at our www site mentioned below.

Figure 3 shows the fraction of early and late type galaxies in 0.5 magnitude bins. While at the bright end ($m_B \lesssim 13.5$) there are fluctuations, due to small number statistics, at fainter magnitudes, the population fractions approach a constant value of about 66% and 32% for late and early type galaxies, respectively.

3. Observations

The acquisition of spectra for the SSRS2 began in 1987. We accumulated data with a variety of telescopes and instrument setups until 1997. In Table 1 we list the different sites, telescopes and detectors. We also list the slit size, wavelength coverage, and the mean resolution of spectra.

In the first observing runs at CASLEO and all observations at Mount Hopkins and the SAAO,

we used Reticon photon-counting devices. The CTIO, ESO, LNA and the 1996 CASLEO spectra are all CCD data.

We reduced the Reticon spectra following the standard procedure (Tonry & Davis 1979). We combined the spectra of each object and then subtracted the sky counts which we observed simultaneously in a separate slit. We then flatfielded the sky-subtracted spectrum to remove detector pixel-to-pixel response. We wavelength calibrated the flatfielded spectrum. The typical error in the polynomial fit for wavelength calibration is ~ 0.3 to 0.4 \AA .

We also reduced the CCD spectra in a standard fashion (*e.g.*, Massey 1992) using IRAF routines. We bias-subtracted, flatfielded, and when necessary, corrected the raw frames for illumination effects. We then extracted the object and comparison spectra using the optimal extraction routines available in IRAF. We did the wavelength using the REDUCER package (provided by W. Wyatt of the CfA), a C language adaptation of the FORTH routines used to reduce the Reticon spectra.

We used the standard cross-correlation technique (Tonry & Davis 1979) and emission line fitting to extract redshifts. For the first CASLEO runs, we used the FORTH version of the cross-correlation code. However, we measured most of our radial velocities using the RVSAO package (Kurtz et al. 1992) in an IRAF environment. We used only two of the default templates supplied with RVSAO: a composite stellar spectrum and a composite galaxy spectrum. Whenever we detected emission-lines, we also used them to measure the redshift. If both cross-correlation and emission-lines provided a radial velocity, we combined these measurements with weights proportional to the estimated uncertainty in each determination (*e.g.*, Tonry & Davis 1979). For velocities with estimated errors below 20 kms^{-1} , usually based on emission lines, we added 25 kms^{-1} in quadrature to account for other sources of systematic errors as suggested by Kurtz and Mink (1998). The internal error in most of our velocities is $\sim 40 \text{ kms}^{-1}$ (*e.g.* da Costa et al. 1984, da Costa et al. 1991).

4. The Catalog

The number of galaxies in the survey is 5426: 3489 are in the southern galactic cap $b \leq -40^\circ$ and $\delta \leq -2.5^\circ$ (1.13 steradians), and 1937 are in the northern galactic cap $b \geq 35^\circ$ and $\delta \leq 0^\circ$ (0.57 steradians). The sample contains objects (836 galaxies, or 15 % of the sample) previously observed for the diameter-limited SSRS (da Costa et al. 1991). We measured 2828 new redshifts or 52% of the sample, including galaxies from a survey of the equatorial region (Huchra et al. 1993).

Tables 2 and 3 contain the SSRS2 catalog. Table 2 contains 5369 galaxies (3439 in the SSRS2 south and 1930 in the SSRS2 north) with $m_{SSRS2} \leq 15.5$. These galaxies constitute a well-defined, magnitude-limited sample for statistical analyses. For each object the entries are: column (1) the galaxy identification in the GSC; column (2) the ESO or MCG identification; columns (3) and (4)

B1950.0 equatorial coordinates; column (5) the m_{SSRS2} magnitude ; column (6) the heliocentric radial velocity v_{\odot} ; column (7) the estimated internal error, ϵ , in the radial velocity; column (8) galaxy morphologies with T types as discussed in Section 2.3; column (9) the source for the radial velocity, where zero represents a value from the literature, and numbers 1 to 9 are the sites in Table 1; column (10) an indicator for galaxies without a radial velocity because of superposed stars (“star”), or because of low surface brightness requiring long integration times (“lsb”); column (11) other identifications for galaxies (e.g. NGC or IC number). Only the first page of Table 2 is shown in this publication. The complete table is available in our www site <http://obsn.on.br/ssrs2>.

Positions are from the GSC, except for those galaxies missed or “merged” into a single object in this catalog. In these cases, the positions, identifications and magnitudes come either from the ESO-LV or MCG catalogs, or are new estimates (16 galaxies mentioned in section 2.1). For other 6 galaxies we also estimated the magnitudes since the quoted value was contaminated by a star image. Magnitudes estimated for these 22 galaxies are labeled with an asterisk. Sources for radial velocities are the same mentioned in da Costa et al. (1991) and for more recent data, the NASA/IPAC Extragalactic Database (NED).

The completeness in radial velocity for galaxies with $m_{SSRS2} \leq 15.5$ in both galactic caps exceeds 99%. We caution users of this catalog that there are 35 galaxies without radial velocities. Of these, 9 are low surface brightness galaxies and 25 have superposed stars which make optical velocities impossible to obtain.

Figure 4 shows the distribution of radial velocities for the SSRS2 north and south subsamples. To compare the samples in a meaningful way, we normalize each distribution by the appropriate survey area. Both subsamples have large amplitude fluctuations. The subsamples differ most noticeably at $\sim 3000 \text{ kms}^{-1}$ and in the redshift range $8000 - 11000 \text{ kms}^{-1}$, where the difference in counts is $\sim 2\sigma$. The clustering of galaxies explains these differences. In the south galactic cap the great nearby void at 3000 kms^{-1} and the Southern wall at 6000 kms^{-1} are prominent structures; the large overdensity in the north cap is due to a structure that extends to 8000 kms^{-1} . Cone diagrams for the two surveys are in da Costa et al. (1994a) and da Costa et al. (1998).

In the early stages of this project (*e.g.*, da Costa et al. 1989) we did not have a proper calibration of the galaxy magnitudes. We thus took a conservative approach when selecting galaxies; we included galaxies from the ESO-LV and MCG catalogs with $m_B \leq 15.5$ as estimated from the MCG magnitudes or from B_T in the case of ESO-LV galaxies. As the m_{SSRS2} magnitudes became available, some of these objects turned out to have $m_{SSRS2} > 15.5$ based on equation (1). We list these 57 objects in Table 3, where the columns have the same meaning as in Table 2.

5. Summary

The SSRS2 catalog, described in this paper, includes 5426 galaxies in the southern hemisphere. For essentially all of these galaxies we present radial velocities, good astrometric positions and

objectively measured magnitudes. The catalog also includes galaxy morphologies compiled from a variety of sources. The magnitude limited sample designed for statistical analyses contains 5369 galaxies brighter than $m_{SSRS2} = 15.5$, distributed within a solid angle of 1.7 steradians, split between two regions in the north and south galactic caps. The magnitude system is homogeneous and equivalent to isophotal, measured at 26 mag arcsec⁻². Its zero-point offset relative to the Zwicky magnitudes, used in the CfA surveys, is estimated to be about 0.1^m.

Since the loss of objects at faint magnitudes, caused by misclassifications of galaxies as stars in the source catalog (GSC), is small, we conclude that the magnitude limited catalog is essentially complete to $m_{SSRS2} = 15.5$. The redshift completeness exceeds 99%. The SSRS2 galaxy catalog is the basis for a variety of studies of large-scale structure either by itself or in combination with the CfA2 to probe larger scales. Together these surveys are the largest database of redshifts of the Local Universe.

The authors thank the time allocation committees of all observatories, for granting this project a generous amount of dark time over a number of years. More recent observations were also made possible thanks to the ESO/Observatório Nacional agreement for shared operation of the 1,52 m ESO telescope at La Silla. The authors thank S. Paoloantonio, C. Valotto and J.H. Calderón for their help in the observations at CASLEO, and M.A. Nunes and D. Nascimento for their help maintaining the ON Reticon in working order. We also thank Will Sutherland, Steve Maddox and Somak Raychaudhuri for providing data from APM surveys. At the CfA, we thank Barbara Elwell for her help in the visual inspection stage of the catalog construction, Susan Tokarz for spectroscopic data reduction, and Cathy Clemens for her help in the use of the ZCAT database.

LNdC appreciates the hospitality of CfA and IAP where part of this work was carried out, and acknowledges support from a CNPq fellowship, the Smithsonian Scholarly Program and the John Simon Guggenheim Foundation. This project has received support from CNPq-NSF (Brazil-USA) and CNPq-CONICET (Brazil-Argentina) bilateral agreements. Partial support has also been provided through CNPq grants 301364/86-9, 453488/96-0 (CNAW), 301373/86-8 (PSP). Additional funds were provided by the Centro Latino-Americano de Física (PSP), FAPERJ (OLC), NSF AST-9023178 (CNAW) and the ESO Visitor Programme (CNAW). The authors acknowledge use of the CCD and data acquisition system supported under U.S. National Science Foundation grant AST-90-15827 to R.M. Rich. This work has made extensive use of the NASA/IPAC Extragalactic Database (NED) which is operated by the Jet Propulsion Laboratory, California Institute of Technology, under contract with the National Aeronautics and Space Administration and of the NASA Astrophysics Data System. This work has also used images from the Digitized Sky Survey, produced at the Space Telescope Science Institute under U.S. Government grant NAG W-2166. The images of these surveys are based on photographic data obtained using the Oschin Schmidt Telescope on Palomar Mountain and the UK Schmidt Telescope.

REFERENCES

- Alonso, M. V., da Costa, L. N., Pellegrini, P. S., & Kurtz, M. J. 1993, *AJ*, 106, 676
- Alonso, M. V., da Costa, L. N., Latham, D. W., Pellegrini, P. S., & Milone, A. E. 1994, *AJ*, 108, 1987
- Barton, E., Geller, M. J., Ramella, M., Marzke, R. O., & da Costa, L. N. 1996, *AJ*, 112, 817
- Benoist, C., Maurogordato, S., da Costa, L. N., Cappi, A., & Schaeffer, R. 1996, *ApJ* 472, 452
- da Costa, L. N., Geller, M. J., Pellegrini, P. S., Latham, D. W., Fairall, A. P., Marzke, R. O., Willmer, C. N. A., Huchra, J. P., Calderon, J. H., Ramella, M. & Kurtz, M. J., 1994a, *ApJ Letters*, 424, L1
- da Costa, L. N., Pellegrini, P. S., Davis, M., Meiksin, A., Sargent, W. L. W., & Tonry, J. L. 1991 *ApJS* 75, 935
- da Costa, L. N., Pellegrini, P. S., Nunes, M. A., Willmer, C. & Latham, D. W. 1984, *AJ* 89, 1310
- da Costa, L. N., Pellegrini, P. S., Sargent, W. L. M., Tonry, J., Davis, M., Meiksin, A., Latham, D. W., Menzies, J. W., & Coulson, I. A. 1988, *ApJ*, 327, 544
- da Costa, L. N., Pellegrini, P. S., Willmer, C., & Latham, D.W. 1989, *ApJ*, 344, 20
- da Costa, L. N., Vogeley, M., Geller, M. J., Huchra, J. & Park, C., 1994b, *ApJ*, 437, 1
- Davis, M., Huchra, J., Latham, D. W., & Tonry, J. 1982, *ApJ*, 253, 423
- da Lapparent, V., Geller, M. J., & Huchra, J. P. 1986, *ApJ*, 302, L1
- de Vaucouleurs, G., de Vaucouleurs, A. 1964, *Reference Catalogue of Bright Galaxies*, (Austin: Univ. of Texas Press)
- El-ad, H., E.-A., Piran, T., & da Costa, L. N. 1996, *ApJ*, 462, L13
- Fairall, A. P., Willmer, C. N. A., Calderón, J. H., Latham, D. W., da Costa, L. N., Pellegrini, P. S., Nunes, M. A., Focardi, P., & Vettolani, G. 1992, *AJ*, 103, 11
- Felten, J. E. 1985, *Comments Astrophys.*, 11, 53
- Geller, M. J., & Huchra, J. P. 1989, *Science*, 246, 897
- Huchra, J. P. 1976, *AJ* 81, 952
- Huchra, J. P. 1996, private communication (ZCAT)
- Huchra, J. P., Latham, D. W., da Costa, L. N., Pellegrini, P. S., & Willmer, C. N. A. 1993, *AJ*, 105, 1637
- Kurtz, M. J. and Mink, D. J. 1998, submitted to *PASP*, astro-ph/9803252
- Kurtz, M. J., Mink, D.J., Wyatt, W. F., Fabricant, D. G., Torres, G., Kriss, G. A., & Tonry, J. L. 1992, in *ASP Conf. Ser. Vol. 25, Proc. 1st Ann. Conf. Astronomical Data Analysis Software and Systems*, ed., D. M. Worrall, C. Biemesderfer, & J. Barnes (San Francisco: ASP), 432

- Lahav, O., et al. 1995, *Science*, 267, 859
- Lasker, B. M., Sturch, C. R., McLean, B. M., Russel, J. L., Jenker, H., & Shara, M. 1990, *AJ*, 99, 2019 (GSC)
- Lauberts, A. 1982, *The ESO/Uppsala Catalogue of the ESO Quick Blue Survey*, (Garching: ESO)
- Lauberts, A., & Valentijn, E. A. 1989, *The Surface Photometry Catalogue of the ESO-Uppsala Galaxies*, (Garching: ESO) (ESO-LV)
- Loveday, J., 1996, *MNRAS*, 278, 1025
- Marzke, R. O., & da Costa, L. N. 1997, *AJ*, 113, 185
- Marzke, R. O., & da Costa, L. N., Pellegrini, P. S., & Willmer, C. N. A. 1998, *ApJ.*, *in press*
- Marzke, R. O., Geller, M. J., Huchra, J. P., Corwin, H. G. 1994*a*, *AJ*, 108, 437
- Marzke, R. O., Geller, M. J., da Costa, L. N., & Huchra, J. P. 1995, *AJ*, 110, 477
- Marzke, R. O., Huchra, J. P., & Geller, M. J., 1994*b*, *ApJ* 428, 43
- Massey, P. 1992, *A User's Guide to CCD Reductions with IRAF* (Tucson: KPNO Computer Support Group)
- Park, C., Vogeley, M. S., Geller, M. J., & Huchra, J. P. 1994, *ApJ*, 431, 569
- Pellegrini, P. S., da Costa, L. N., Huchra, J. P., Latham, D. W., & Willmer, C. 1990*a*, *AJ* 99, 751
- Pellegrini, P. S., Willmer, C. N. A., da Costa, L. N., & Santiago, B. X. 1990*b*, *ApJ*, 350, 95
- Raychaudhury, S., Lynden-Bell, D., Scharf, C. & Hudson, M. J. 1994, *Bull American Astron. Soc.*, 184, # 38.06
- Ramella, M., Geller, M. J., & Huchra, J. P. 1992, *ApJ*, 384, 396
- Ramella, M., Pisani, A., & Geller, M. J. 1997, *AJ*, 113, 483
- Ramella, M., Girardi, M., da Costa, L. N., & Geller, M. J. 1998, *in preparation*
- Schechtman, S. A., 1996, Landy, S. D., Oemler, A., Tucker, D. L., Lin, H., Kirshner, R. P., & Schechter, P. L. 1996, *ApJS*, 47, 172
- Tonry, J., & Davis, M. 1979, *AJ*, 84, 1511
- Vorontsov-Velyaminov, B. A., & Arkhipova, V. P. 1963-1968, *The Morphological Catalogue of Galaxies*, (Moscow: Moscow University Press), Parts 2-4 (MCG)
- Willmer, C. N. A., da Costa, L. N., Pellegrini, P. S., Latham, D. W., & Freudling, W. 1995, *AJ*, 109, 61
- Willmer, C. N. A., da Costa, L. N., Pellegrini, P. S. 1998, *AJ*, 115, 869
- Zwicky, F., Herzog, E., Wild, P., Karpowicz, M, & Kowal, C. T. 1961-1968, *Catalogue of Galaxies and Clusters of Galaxies*, (Pasadena: Caltech), vol I-VI

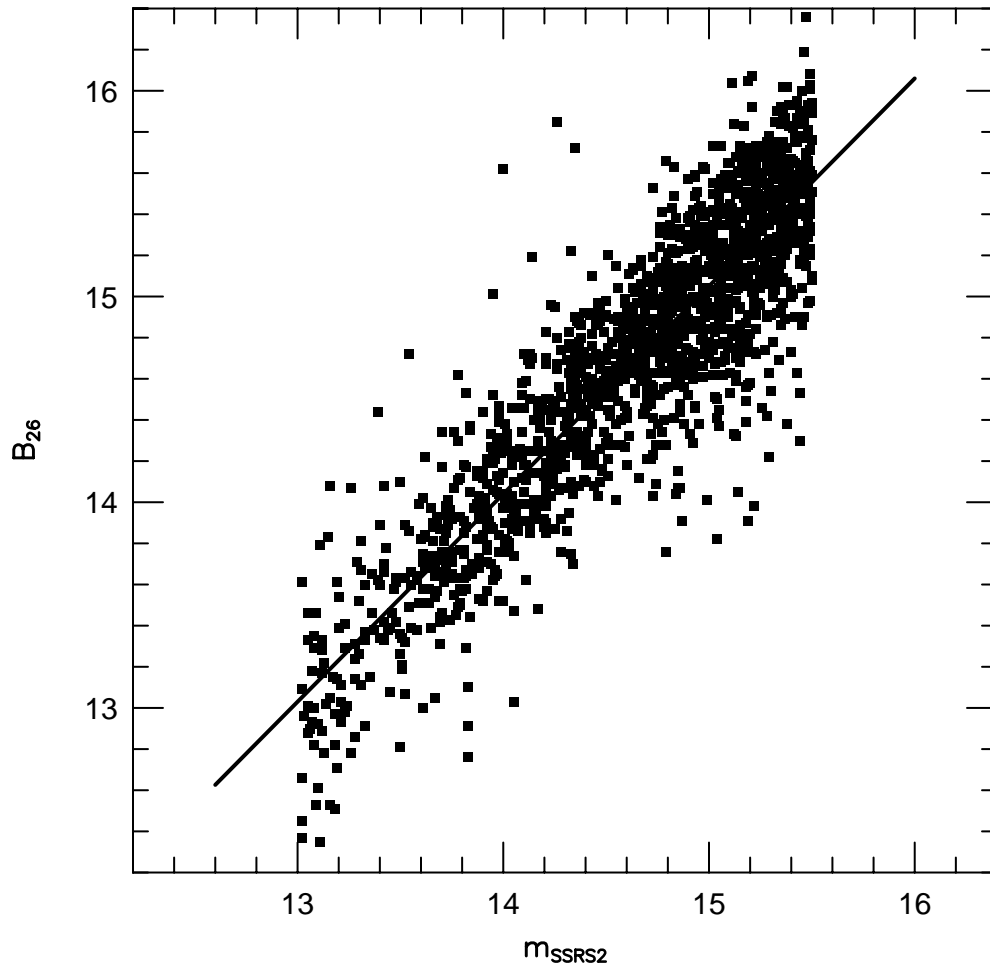


Fig. 1.— Comparison of galaxy magnitudes in our catalog, m_{SSRS2} , with B_{26} from the ESO-LV catalog for 1588 objects in common between the two data sets. The line represents a linear square fit to the data points as discussed in the text.

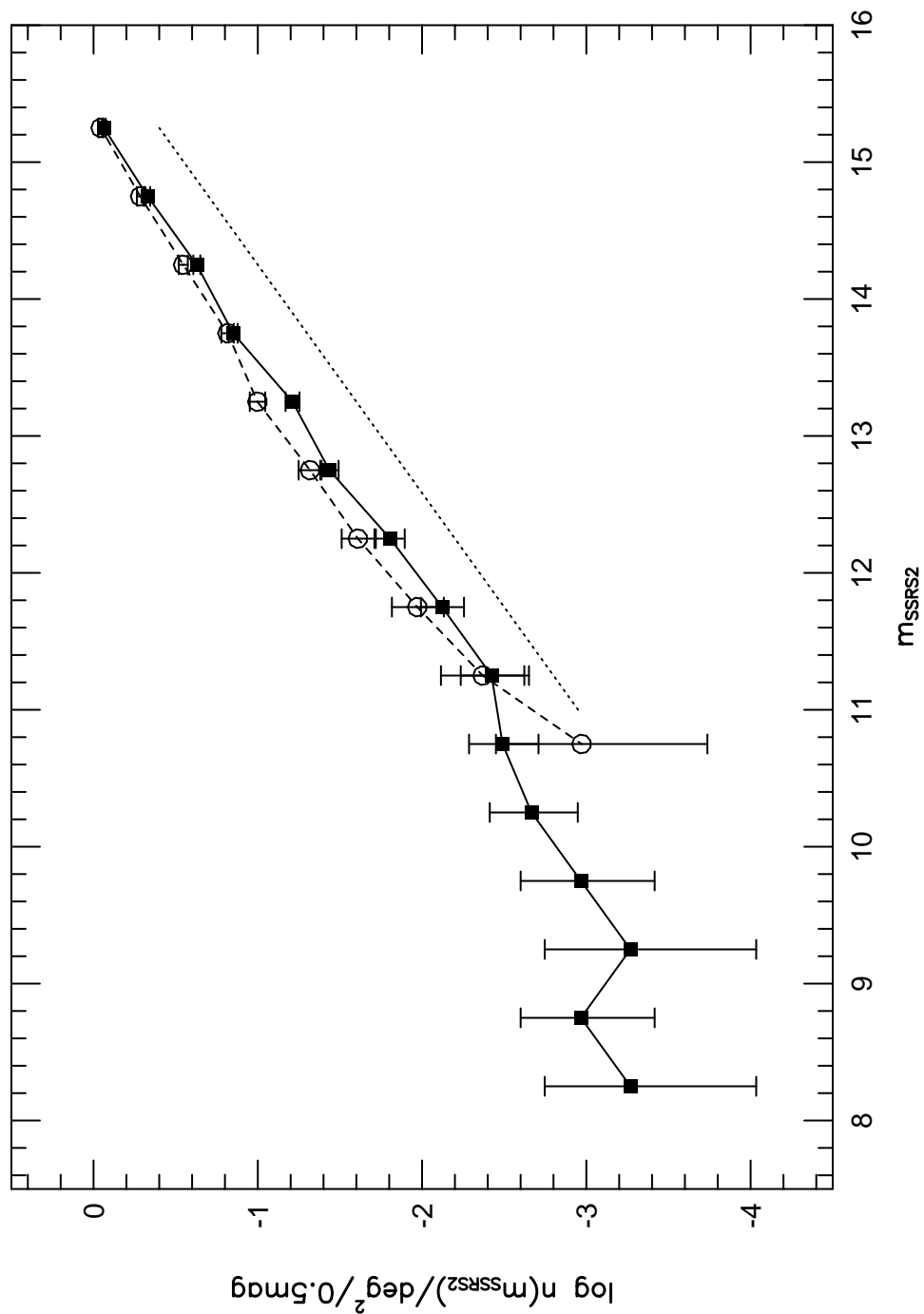


Fig. 2.— Number counts in galaxies per square degree in 0.5^m bins for the SSRS2 south (squares) and north (circles) subsamples. For comparison we show a line with slope equal to 0.6 expected for a homogeneous distribution with an arbitrary normalization.

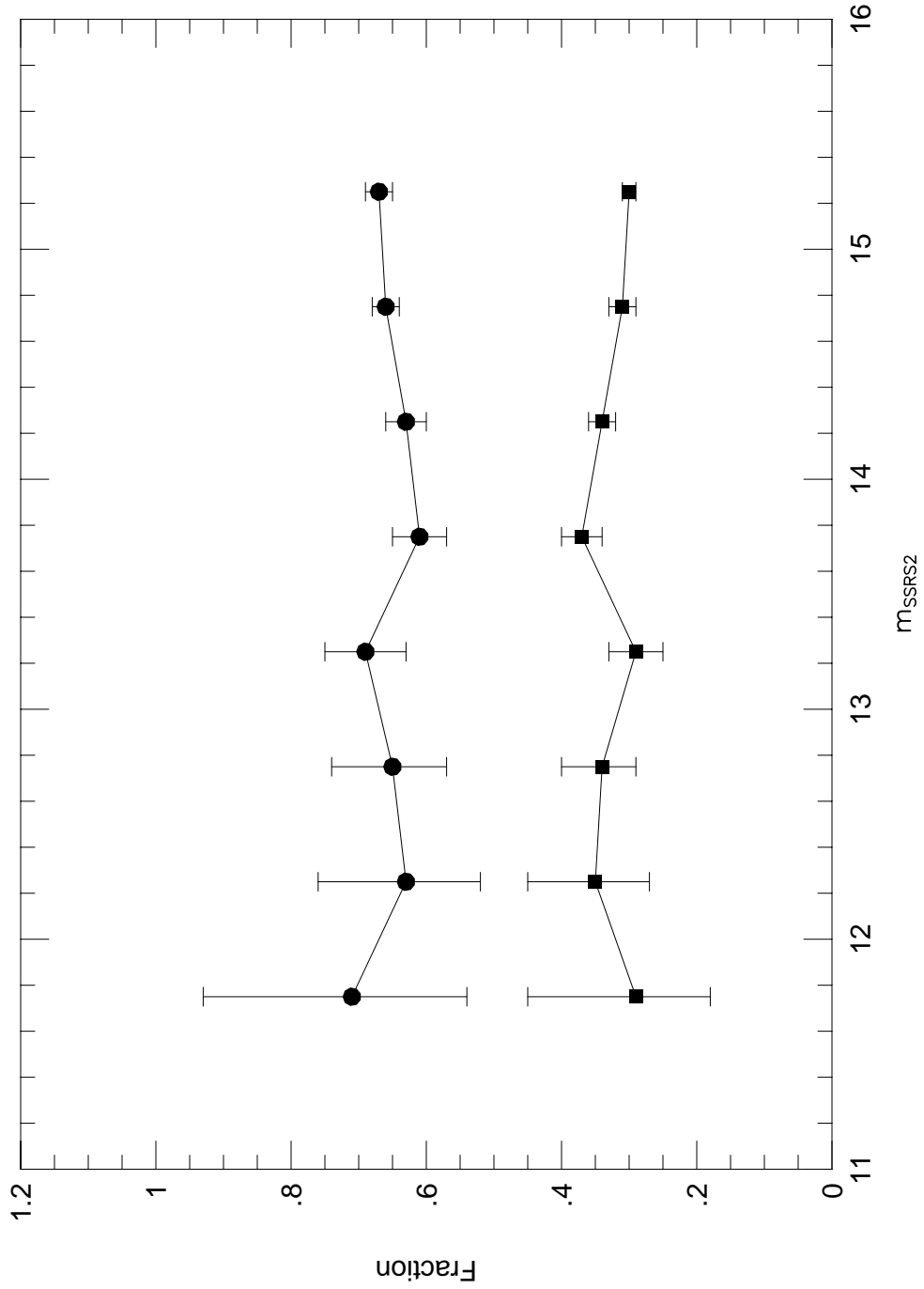


Fig. 3.— Distribution in 0.5^m bins of the fraction of different morphologies in the SSRS2. Late type galaxies ($1 \leq T \leq 9$) are shown as full circles, while early-type galaxies ($-5 \leq T \leq 0$) are shown as full squares.

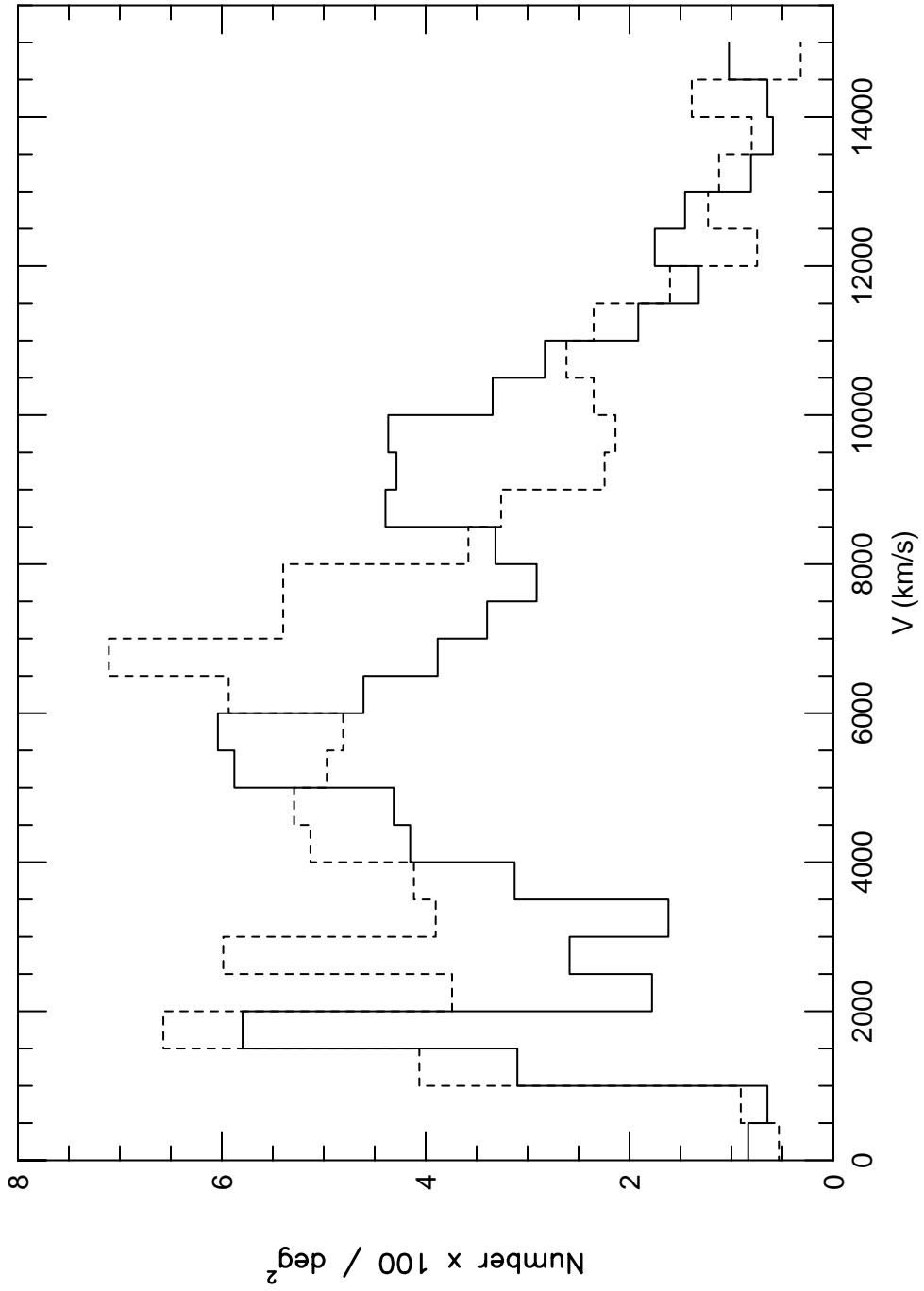


Fig. 4.— Distribution of the SSRS2 subsamples in radial velocity using 500 km s^{-1} bins. The solid line represents the SSRS2 south sample while the dashed line represents the SSRS2 north.

TABLE 1. Observational setups

Site	Code	telescope size m	detector	detector size pixels	pixel size μm	slit width <i>arcsec</i>	Wavelength range \AA	FWHM \AA
CTIO	1	1.50	GEC CCD	1024	22	2	4500-7000	8
CASLEO	2	2.15	Reticon	2048	15	3×12	4400-7200	6
CASLEO	3	2.15	Tek CCD	1024	22	3	4800-6800	6
ESO	4	1.52	Ford CCD #27	2048	22	2.5	3700-7000	4
ESO	5	1.52	Ford CCD #24	2048	22	2.5	3700-7000	4
ESO	6	1.52	Loral CCD #39	2048	22	2.5	3700-7000	4
SAO	7	1.50	Reticon	2048	15	3×12	4800-6800	6
LNA	8	1.60	EEV CCD	1024	22	3.0	4800-6900	6
SAAO	9	1.90	RPCS	2048	15	3×12	3400-5200	6

TABLE 2. Catalog of Galaxies in the SSRS2 Sample (first page only)

GSC	ESO/MCG	α	δ	m_{SSRS2}	v_{\odot}	ϵ	T	Site	Note	NGC/IC
(1)	(2)	1950.0	1950.0	(5)	kms^{-1}	kms^{-1}	(8)	(9)	(10)	(11)
4666.0499	-0101024	00:00:01.1	-03:59:22	14.49	6474	30	7	0		
4666.0416	-0101025	00:00:14.9	-03:53:04	15.19	6202	32	5	7		
6992.0319	349 G 21	00:00:20.8	-34:30:50	13.86	6845	39	4	8		N 7812
6995.1144	349 G 22	00:00:39.5	-36:12:56	15.15	14935	38	-2	8		
6415.0273		00:00:40.9	-27:31:10	15.31	8993	35	5	1		
5263.0658	-0201012	00:00:48.6	-11:02:56	14.92	9029	37	5	0		
5263.0881	-0201013	00:00:58.5	-11:01:22	14.47	8922	25	-2	0		N 7808
5266.0282	-0301016	00:01:11.5	-14:58:21	15.18	5842	37	5	0		
5263.0979	-0201015	00:01:27.7	-11:27:12	15.04	11360	39	5	0		
5263.0360	-0201016	00:01:35.6	-12:15:44	15.00	9042		5	0		I 5384
5266.0743	-0301017	00:01:38.5	-14:48:07	15.13	7301	54	5	1		
6418.1203	409 G 10	00:01:44.1	-30:10:02	15.41	19136	76	6	1		
5260.0347	-0201017	00:01:48.1	-08:19:18	15.38	8645	43	-2	7		
	-0101028	00:02:03.0	-07:21:30	13.50	3814	29	5	0		
5260.0548	-0101030	00:02:06.2	-08:22:43	14.24	8584	23	-5	0		
6989.0634	409 G 12	00:02:09.0	-30:45:44	14.48	7985	33	-5	8		
5838.0144	-0301018	00:02:12.4	-16:18:32	15.06	10136	35	5	8		
4666.0559		00:02:22.1	-04:08:44	15.09	7851	36	5	7		
6989.0622	409 G 13	00:02:26.5	-30:47:03	15.15	8181	35	-1	8		
4669.0413		00:02:31.7	-07:22:19	13.72	3868	36	5	7		
6995.1014		00:02:33.6	-35:58:24	14.72	8575		-5	0		
5263.0914	-0201019	00:02:39.7	-11:46:52	14.34	6772	33	-2	2		I 1529
5838.0651	-0301019	00:02:43.3	-16:45:18	13.77	7397	38	5	8		N 7821
6418.0423	409IG 15	00:02:59.0	-28:22:39	15.38	697	29	4	1		
6995.1135	349 G 25	00:03:08.7	-36:13:44	14.88	8307	39	3	2		
6989.0822	409 G 16	00:03:23.1	-31:22:51	15.20	7826	37	1	2		
4666.0842		00:03:23.9	-03:55:18	15.44	6568	46	-2	7		
6995.0746	349 G 27	00:03:25.9	-36:24:54	15.07	8385	53	2	0		
6989.0909	409 G 18	00:03:31.1	-30:54:25	15.31	8812	40	1	2		
6412.0162	472 G 14	00:03:39.3	-23:07:51	15.18	8160	35	3	0		
5266.0550	-0201025	00:03:53.6	-13:41:40	14.72	5800	50	15	0		N 7828
4666.0375	-0101033	00:03:54.8	-03:59:41	13.89	6204	22	-2	0		N 7832
6989.0262	409 G 19	00:03:56.8	-32:14:05	15.06	7783	47	3	2		
6415.1110		00:04:10.3	-25:21:29	14.98	10095	32	5	1		
5844.0284	538 G 22	00:04:37.1	-22:03:53	14.84	10138	44	2	0		
6418.0692	409IG 21	00:04:48.0	-28:23:49	15.32	18048	54	1	1		
6995.0409	293 G 38	00:04:53.5	-37:43:42	15.14	8400	41	4	2		
5844.1032	538 G 23	00:04:57.9	-21:00:35	15.32	19602	35	1	8		
6418.0253	409 G 22	00:05:48.2	-30:11:38	15.19	1518	43	6	8		N 7
5263.0636	-0201028	00:06:00.9	-11:13:39	15.10	9159	43	5	0		
6992.0263	349 G 32	00:06:02.2	-34:08:11	13.19	6813	36	4	8		
4669.0736	-0101036	00:06:02.2	-05:29:44	15.23	11751	43	5	7		N 10
4669.0147	-0101037	00:06:10.0	-07:16:31	14.87	8333	37	-2	0		
5260.0239		00:06:24.2	-08:52:52	15.23	5447	39	5	7		
6995.0346	293 G 42	00:06:25.9	-37:36:29	15.31	8703		1	0		
6992.0598	349 G 33	00:06:31.0	-33:11:32	14.64	6896	37	3	8		
6995.0358	293 G 43	00:06:35.1	-37:38:09	15.06	8697	39	-5	2		
4669.0119	-0101040	00:06:37.4	-07:12:12	15.11	12076	36	5	7		
7523.0159		00:06:58.2	-37:49:51	14.42	8686		5	0		

TABLE 3. Galaxies fainter than $m_{SSRS2} = 15.5$

GSC	ESO/MCG	α	δ	m_{SSRS2}	v_{\odot}	ϵ	T	Site	Note	NGC/IC
(1)	(2)	1950.0	1950.0	(5)	kms^{-1}	kms^{-1}	(8)	(9)	(10)	(11)
6416.0784	472IG 21	00:10:47.9	-26:52:15	15.98	17122	40	0	5		
5843.0614	539 G 8	00:19:05.7	-19:57:21	15.68	7552	39	-5	8		
5840.0845	-0302015	00:26:36.2	-16:07:38	16.52	19475	25	5	2		
5840.0285	-0302018	00:27:58.3	-16:58:05	15.62	10361	40	5	2		
5847.0359	540 G 17	00:41:51.9	-17:37:28	15.78	9305	47	15	8		
5847.0346	540 G 17 A	00:41:53.0	-17:37:40	16.64	9009	38	-5	5		
5853.0024		01:08:27.2	-19:13:41	15.70	16057		5	9		
7004.1897	352 G 37	01:15:48.0	-36:46:08	15.61	7178	33	2	2		
5851.1354	-0304039	01:16:15.3	-17:18:46	15.66	9275	48	5	2		
7004.0581	352 G 76	01:23:33.7	-34:45:01	15.55	14891	38	0	8		
4684.0326N		01:23:49.3	-07:44:00	16.50*	14453	27	-5	5		
5854.1961	476 G 14	01:27:16.6	-22:34:44	16.97	5835	40	2	5		
5854.1325	542 G 23	01:29:56.0	-21:05:08	15.75	15841	34	-3	5		
6429.0182	477 G 2	01:42:35.3	-23:10:10	15.90	12017	39	-2	5		N 667
5862.1784	545 G 42	02:37:10.8	-20:03:22	16.01	4692	55	-2	8		
5866.0062	546 G 5	02:39:03.8	-18:08:57	16.29	7853	43	6	8		
5869.0876	546 G 7 A	02:39:33.1	-21:01:29	17.35	7784	29	6	5		
5869.0408	546 G 9	02:39:40.2	-21:29:58	16.90	2928	40	7	5		
7011.1032	416 G 21	02:45:00.4	-31:41:36	15.75	7460	38	1	2		
6437.0010	480 G 3	02:45:53.0	-22:57:45	15.59	4667	35	1	1		
5886.0493	546 G 24	02:45:57.8	-18:11:42	15.78	4314	29	-1	3		N 1119
5867.0382	546 G 28	02:51:05.5	-17:48:19	15.55	11022	39	3	8		
5870.0700	546 G 32	02:53:49.3	-22:27:14	15.51	8105	39	1	1		
7025.0725	357 G 1	03:00:10.1	-35:52:56	16.49	4391	47	7	9		
6438.0866	480 G 20	03:00:14.6	-22:59:48	15.62	1439	29	6	1		
5871.0030	547 G 4	03:01:14.6	-20:22:13	15.59	3322	40	3	8		
5871.0462	547 G 7	03:01:31.2	-22:26:55	15.72	4327	25	10	1		
4710.0335	-0109009	03:06:41.6	-04:06:18	16.14	8374	56	5	7		
5874.0691	548 G 46	03:32:21.4	-17:38:27	16.04	1625	29	2	5		
7034.0090		03:40:10.8	-36:58:13	15.70	15069	46	5	1		
7570.1475	302 G 12	03:48:43.3	-39:31:32	16.43	5299	25	7	5		
6455.0650	483IG 1	03:54:38.4	-24:38:29	15.82	4203	29	15	1		
7036.0846	359IG 14	04:01:13.6	-36:16:48	15.75	17642	48	-2	1		
7578.0532	303 G 5	04:12:12.0	-38:13:22	15.72	14934	41	-4	2		
6463.0040	420 G 20	04:23:01.3	-29:20:48	16.10	22079	44	1	5		
5524.0949		12:00:38.7	-14:21:57	16.50	3969	33	-2	5		
6118.0288	575 G 60	13:05:12.0	-20:43:15	16.26	12454	29	3	8		
6113.1129		13:14:57.0	-15:03:12	16.61	15047	75	6	1		
6130.0412N		13:41:05.1	-19:34:23	15.80*	9781	56	-5	5		
6130.0412S		13:41:05.8	-19:34:34	15.80*	9740	48	-5	5		
4974.0895S	-0135021E	13:52:57.6	-05:43:45	16.50*	2034	52	15	0		
6149.0229	578 G 21	14:02:43.2	-22:00:04	15.79	14384	32	-2	8		
7965.0990	341IG 31	20:59:42.2	-38:10:52	15.67	13443	33	-1	1		
5806.0142	-0256020	22:08:02.0	-10:42:39	16.56	15815		23	9		
6962.0813	533 G 20	22:19:46.4	-23:46:38	15.90	11611	39	-2	8		
7996.0045	345 G 9	22:22:11.0	-38:08:35	16.16	11092	43	5	8		
6965.0915		22:22:42.2	-25:35:42	16.00	16394	62	-1	1		
7997.0783	345 G 17	22:28:13.2	-38:17:02	15.61	21952	39	-4	8		
7997.0836	345 G 28	22:31:21.7	-38:25:19	15.67	9131	47	-1	1		
5817.0253	-0257018	22:32:09.0	-13:10:17	16.00	4977	39	5	8		

TABLE 3. (continued)

GSC	ESO/MCG	α	δ	m_{SSRS2}	v_{\odot}	ϵ	T	Site	Note	NGC/IC
(1)	(2)	1950.0	1950.0	(5)	kms ⁻¹	kms ⁻¹	(8)	(9)	(10)	(11)
6966.1251	534 G 12 A	22:36:28.6	-26:06:33	16.73	8082	30	3	1		
7512.1134	407 G 4	23:03:42.2	-36:30:54	16.05	2854	47	10	9		
8013.1334		23:20:06.7	-38:10:08	17.00	15829	36	5	2		
7521.1084	408IG 17	23:39:11.0	-36:54:12	15.86	11722	41	23	1		
6987.0220	471 G 11 A	23:43:47.0	-28:16:51	15.94	8673	49	-5	1		
7516.0327	471 G 36	23:50:37.2	-31:59:59	15.56	14578	38	-2	8		
6995.0970	349 G 18	23:59:00.3	-36:35:43	15.58	14682	36	0	8		